

Identification of Dynamic Rollover Precursors for Enhanced Helicopter Flight Data Monitoring (HFDM) Applications

Ilias Baali

Graduate Research Associate
Georgia Institute of Technology
Atlanta, GA, USA

Alexia P. Payan

Research Engineer
Georgia Institute of Technology
Atlanta, GA, USA

Charles C. Johnson

Research Engineer/Program Manager
Federal Aviation Administration
Atlantic City, NJ, USA

Dimitri N. Mavris

S. P. Langley NIA Distinguished Professor
Georgia Institute of Technology
Atlanta, GA, USA

ABSTRACT

Dynamic rollovers represent a major hazard for helicopters during near-ground operations, often resulting in significant aircraft damage and passenger injuries. To improve safety in operations, recent studies have focused on developing a Helicopter Flight Data Monitoring framework to provide data-driven insights on operational safety. This work contributes to that effort by proposing an approach to identify precursors to dynamic rollovers. According to NTSB reports, approximately 60% of such incidents occur during in-flight phases like hover, hover-taxi, or landing. To capture the complex non-linear dynamics of helicopters, physics-based simulations were conducted to estimate a first hitting time metric, defined as the time until blade-ground contact, across a wide range of initial conditions for an in-flight initial state of the helicopter. Eight parameters were identified as driving the first hitting time, and a probabilistic model was created to predict the distribution of that metric for different values of those parameters. Based on the predicted distributions, a risk-based metric was derived to robustly assess the risk of dynamic rollover and identify safer operational boundaries.

NOTATION

CI_α	Confidence interval at confidence level α
h	Initial height of the helicopter (ft)
T	First hitting time (s)
V_x	Longitudinal speed of the helicopter (kt)
V_y	Lateral speed of the helicopter (kt)
X_a	Lateral cyclic control input (%)
X_b	Longitudinal cyclic control input (%)
X_c	Collective control input (%)
μ	Mean parameter of the lognormal distribution
ϕ	Orientation of the ground slope relative to the helicopter (deg)
σ	Standard deviation parameter of the lognormal distribution
θ	Model parameters

INTRODUCTION

According to the Helicopter Flying Handbook, dynamic rollovers occur when a helicopter “starts to pivot laterally around its skid or wheel”, (Ref. 1). Since 2008, the National Transportation Safety Board (NTSB) has investigated 128 accidents related to dynamic rollovers in the United States. Approximately half of these accidents resulted in some level of

injuries, with about 11% resulting in serious injuries to the pilot or their passengers. All of these accidents caused substantial damage to the structure and engine of the helicopter, which made the aircraft unusable after the fact. Dynamic rollovers can occur during any near-ground operation: the NTSB data highlights that 39% of the accidents occurred during take-off, 33% during hover (including hover taxi), and 28% during landing. During these phases of flight, a drift of the helicopter, caused by a wind gust, for example, can result in a dynamic rollover if the skids and/or wheels were to hit the ground. For the landing phase, an excessive vertical speed combined with sloping ground could also result in the creation of an excessive roll rate, eventually leading to a dynamic rollover.

It is worth noticing that most of the accidents reported in CAROL, the NTSB’s database access tool, happened during flight training with student pilots on board. The main cause was either pilot error or a lateral wind gust that created a drift and roll of the helicopter, resulting in a dynamic rollover before the flight instructor could react. This shows the importance of being able to quickly detect and identify the conditions leading to dynamic rollovers, in order to warn pilots of the scenarios most likely to result in a dynamic rollover, thus preventing their occurrence. The goal of this study, therefore, is to identify precursors in flight data to assess, in real time or *a posteriori*, the risk of a dynamic rollover based on the current state of the helicopter.

Presented at the Vertical Flight Society’s 81st Annual Forum & Technology Display, Virginia Beach, VA, USA, May 20–22, 2025. Copyright © 2025 by the Vertical Flight Society. All rights reserved.

BACKGROUND

In recent years, several studies have focused on developing an integrated flight data monitoring framework to improve safety in helicopter operations (Ref. 2). The objective of these studies was to leverage helicopter flight data monitoring (HFDM) to uncover patterns in flight data and better understand (Ref. 3) routine operations, as well as to detect anomalies within these patterns to reveal and mitigate potentially unsafe situations (Ref. 4) (Ref. 5). This work builds on this effort with the goal of mitigating the risk of dynamic rollovers through HFDM. Specifically, the team decided to expand on the methodology presented in Alek Gavrilovski’s thesis (Ref. 6), in which the author provides a way to enhance existing helicopter flight data monitoring (HFDM) systems by using physics-based models. Instead of analyzing safety events within flight records using only directly measured variables, a metric of interest is derived from these measurements by applying an appropriate model of the helicopter’s dynamics. In the case of dynamic rollovers, that metric of interest is the ‘first hitting time’, the time delay that it would take for the helicopter blades to hit the ground from the current state of the helicopter. The model used to derive this metric can either be a 2D or 3D model derived from the equations of motion and flight dynamics, or it can be created from simulation data gathered with a high-fidelity simulation software like FlightLab. This second option has been found to yield better results and was therefore chosen for this study.

METHODOLOGY

In this section, we describe the approach that we followed to derive a robust metric assessing the risk of dynamic rollovers from an initial near-ground state of the helicopter.

Scenario definition

We start by defining a few specific scenarios for which to analyze the risk of dynamic rollovers. Based on the findings of the NTSB accident reports, four key scenarios were identified:

- A scenario simulating the takeoff phase, with the helicopter starting from the ground and taking off vertically to a steady hover.
- A hover scenario simulating hover practice during flight training, as most accidents during this phase of flight are caused by student pilots overcontrolling the aircraft.
- A hover taxi scenario where the helicopter is taxiing over a taxiway, potentially making turns by applying pedals and lateral cyclic inputs.
- A landing scenario starting from a hover phase, performed at various vertical and horizontal speeds.

For this study, we decided to focus on the three latter scenarios, which were grouped together as an “in-flight” scenario for which the helicopter is initially located a few feet above

Table 1: Variable ranges used to create the DOE for the “in-flight” scenario.

Parameter	Min Value	Max Value
Initial height h (ft)	5	50
Roll rate p (deg/s)	-45	45
Pitch rate q (deg/s)	-45	45
Yaw rate r (deg/s)	-45	45
Forward velocity V_x (kt)	-35	35
Lateral velocity V_y (kt)	-35	35
Vertical velocity V_z (ft/min)	-500	500
Wind azimuth $Wind_{az}$ (deg)	0	360
Wind magnitude $Wind_h$ (kt)	0	25
Ground slope (deg)	0	25
Slope orientation ϕ (deg)	0	360
Lateral cyclic X_a (%)	-30	30
Longitudinal cyclic X_b (%)	-30	30
Collective input X_c (%)	-30	30
Pedals input X_p (%)	-30	30

ground, as opposed to the takeoff scenario for which the helicopter starts from the ground. To encompass the three selected cases, a wide range of initial states was analyzed through physics-based simulations, as described below.

Simulations

For each one of the scenarios, we created a design of experiments (DOE) (Ref. 7) to identify an optimal set of simulations to extract information on the first hitting time for various initial states in the “in-flight” scenario. A wide range of values was identified for each variable, and a space-filling design was used to generate the optimal combinations of parameters and keep the number of experiments to a minimum. Considering the computational cost of each FlightLab simulation, 28,000 combinations of inputs were kept to create the DOE. The variables used to define each simulation and their associated ranges are presented in Table 1.

For each case, the helicopter’s dynamics were simulated for 10 s using FlightLab and the time it took for the helicopter blades to touch the ground was recorded.

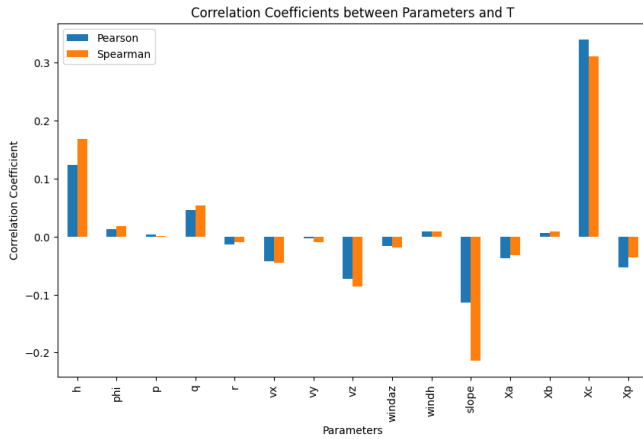


Figure 1: Correlation coefficients between each parameter and the first hitting time T .

Parameters importance

Once the first hitting time has been extracted for each simulation, the individual impact of each parameter on that value can be analyzed. The objective is to identify which variables impact the most the first hitting time and are therefore more critical in the identification of dynamic rollover situations.

Correlation coefficients First, we analyzed the correlation coefficients between each parameter and the first hitting time T to identify potential linear (Pearson coefficients) and/or monotonic (Spearman coefficients) relationships. These coefficients are shown in Figure 1. As one can notice, the collective input is the most correlated to T , followed by the ground slope angle and the initial height of the helicopter. However, parameters such as the roll and yaw rates, lateral velocities, or wind parameters have no direct correlation to the output. This is expected as the impact of these variables is closely related to the value of other parameters. For instance, a left lateral velocity will increase the first hitting time if it corresponds to a motion towards the downslope direction whereas it would significantly decrease it otherwise, as the helicopter would be flying into the ground. This shows the need to further analyze the impact of individual parameters through additional metrics.

Feature importance To further analyze the impact of individual parameters, a random forest model was created. Random forests (Ref. 8) are ensemble-based classification models used to predict categorical classes based on a set of input values. For the purpose of analyzing the impact of the initial parameters on the first hitting time, each simulation was labeled as “safe” or “unsafe” based on the corresponding T value. An arbitrary threshold of 2.5 s was selected for this labeling, with cases for which $T \leq 2.5$ s classified as “safe”. It is important to understand here that this threshold alone is not sufficient to assert that a situation is actually safe or unsafe with regard to dynamic rollovers. Instead, this threshold is merely used as

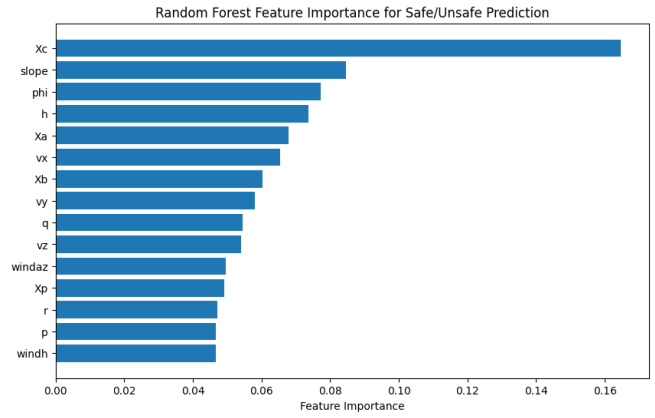


Figure 2: Random Forest feature importance.

an indication that a specific set of initial conditions will result in a low or high value of the first hitting time. A useful feature of random forest models is the ability to calculate *feature importance* (Ref. 9), a metric that determines how much each variable contributes to the choice of the output label in the model. The results are shown in Figure 2. Once again, the collective input X_c is identified as the most important variable to estimate the magnitude of the first hitting time. To a lesser extent, the slope parameters (magnitude and orientation ϕ) and the height h are also identified as important parameters. Compared to the correlation analysis, the lateral cyclic X_a and longitudinal cyclic X_b , also appear to have a significant impact with respect to dynamic rollovers. This is an expected result that also illustrates the point made in the previous paragraph regarding the insufficiency of correlation coefficients to identify relevant parameters. However, feature importance does not seem to identify any variable as significantly less important than the others, as most parameters have a relatively similar impact on the first hitting time output.

SHAP values Another useful metric for identifying the impact of the different inputs on the predicted first hitting time output is the SHAP values (Ref. 10). SHAP values estimate the deviation from a baseline (in our case, the average first hitting time in the data) caused by each parameter. As shown in Figure 3, the first 8 parameters identified as having the most significant impact on T are similar to the ones found with importance feature, with a few variations in their ranking.

Probabilistic modeling

In order to further analyze the impacts of the different variables, a surrogate model of the first hitting time was created. This model has multiple purposes: first, it enables the quick estimation of the first hitting times, without needing to run a whole simulation in FlightLab. This is a critical capability for Helicopter Flight Data Monitoring applications as the amount of flight data to analyze will not allow for a complete simulation for each data point. Having an accurate surrogate model also enables real-time monitoring of the risk of dynamic rollovers. Moreover, a surrogate model makes it possi-

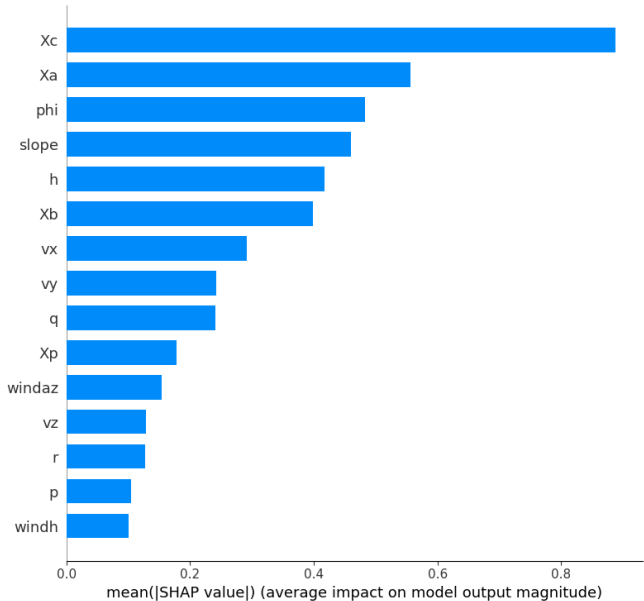


Figure 3: SHAP values.

ble to analyze the variability of the first hitting time for various values of the input variables, by enabling the use of Monte-Carlo simulations.

A difficulty for creating a good surrogate model of the first hitting time value resides in the highly non-linear nature of the simulations. Because of the complex dynamics of the helicopter, small changes in initial conditions lead to high variations in first hitting time, making it complicated to create a good regression model using artificial neural networks, especially considering that the amount of training data from simulations is limited by computational resources. Thus, a different approach was used to create a good predicting model.

Instead of predicting the exact value of the first hitting time for each set of initial conditions, we decided to explore a probabilistic interpretation of the problem. Our goal was to estimate the distribution of first hitting time values for specific conditions, which would provide information on both the expected value and potential deviations, enabling a more robust analysis of the risk for each situation. In order to create such a model, a log-normal distribution was chosen for the output distribution, the parameters of which are calculated using a neural network model trained on the FlightLab simulation data. We created a fully-connected network with 5 hidden layers of sizes 256, 128, 64, 32, 16, and a ReLU activation function. The model outputs two parameters, the mean of the log-first hitting time as well as the logarithm of standard deviation for the log-first hitting time. Taking the exponential of the latter would yield the standard deviation of the distribution, effectively enforcing the non-negativity of this parameter. The structure of the model is summarized in Table 2.

The 8 most important variables identified in the previous section were retained as model inputs, reducing the network’s size and increasing the diversity of the training data.

This neural network was trained using Maximum Likelihood Estimation, which identifies the distribution most likely to

Table 2: Summary of the neural network architecture.

Property	Description
Number of layers	5 hidden layers
Hidden sizes	[256, 128, 64, 32, 16]
Inputs	8 inputs
Outputs	- mean μ - standard deviation $\log \sigma$

have generated the observed data by minimizing the negative log-likelihood. For a continuous variable, the log-likelihood function is given by

$$\log \mathcal{L}(\theta) = \sum_{y_i} \log p(y_i | \theta) \quad (1)$$

where θ represents the model parameters, and y_i represents the observed data. Here, the specificity is that the distribution p is conditioned on the log-normal parameters $\mu_\theta(x_i)$ and $\sigma_\theta(x_i)$ given by the neural network. Thus, the training objective for our problem becomes

$$\max_{\theta} \mathbb{E}_{(x_i, T_i)} [\log p(T_i | \mu_\theta(x_i), \sigma_\theta(x_i))] \quad (2)$$

Another difficulty is the limited time horizon of the simulations used to acquire the training data. Indeed, the FlightLab simulations were set to simulate the dynamics of the helicopter within a fixed time horizon of 10 s. Therefore, cases for which the helicopter did not crash within the first 10 s of simulation resulted in the same first hitting time value of 10 s, providing an inaccurate representation of the first hitting time distribution. This is a case of right censoring, where the actual information given by T is that the crash did not occur within the first 10 s, i.e., $T_i \geq 10$ s. To account for right censoring in the training objective, the log-likelihood loss was modified to include the survival function $p(T_i \geq 10 \text{ s})$ for the censored cases. Thus, the new objective becomes

$$\max_{\theta} \left(\mathbb{E}_{(x_i, T_i) \text{ uncensored}} [\log p(T_i | \mu_\theta(x_i), \sigma_\theta(x_i))] + \mathbb{E}_{(x_i, T_i) \text{ censored}} [\log p(T \geq 10 \text{ s} | \mu_\theta(x_i), \sigma_\theta(x_i))] \right). \quad (3)$$

The neural network summarized in Table 2 was trained using the above objective.

To compensate for the unbalanced distribution of output values in the training data, shown in Figure 4, we decided to train the model using mini-batches randomly sampled from a weighted distribution. The weight attributed to each data point (shown in red in Fig. 4) is based on the value of the first hitting time, and ensures that the output values T_i are uniformly distributed in each batch. Doing so improved the fitting performance across the whole range of first hitting time values.

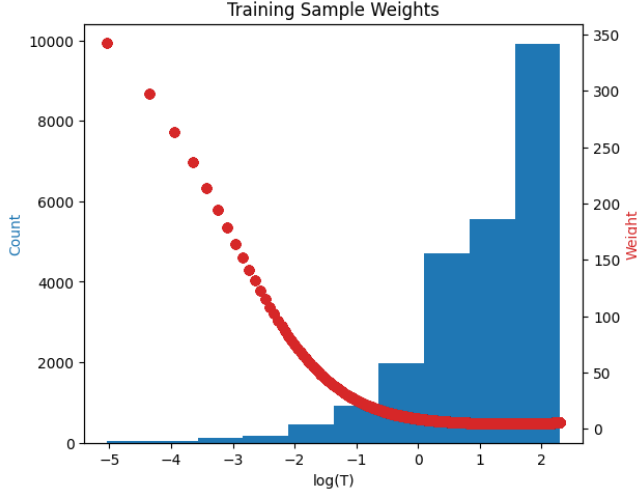


Figure 4: Distribution of $\log(T)$ (in blue) and corresponding weights used for mini-batch sampling (in red).

Goodness of fit

Once the model trained, we analyzed the goodness of fit of the distribution. Noting that

$$X \sim \text{LogNormal}(\mu, \sigma^2) \Leftrightarrow \log X \sim \mathcal{N}(\mu, \sigma^2)$$

we tested the predicted distributions for $\log T$ against a normal distribution.

Standardized Residuals Since the parameters (μ, σ) depend on the input values and are inferred by the model, we started by calculating the standardized residual z_i for each data point according to

$$\log T_i \sim \mathcal{N}(\mu(x_i), \sigma^2(x_i)) \Leftrightarrow z_i = \frac{\log T_i - \mu(x_i)}{\sigma(x_i)} \sim \mathcal{N}(0, 1).$$

The standardized residuals for the test set are plotted in Figure 5. We can notice that they closely follow the standard normal distribution, which suggests a good fit of the distribution parameters from the neural networks. For a more formal evaluation of the closeness between the two distribution, we used a Kolmogorov-Smirnov statistic test to evaluate the null hypothesis that the samples were drawn from the standard normal distribution. We obtained a p-value of $0.286 \gg 0.05$, suggesting that there is no statistical evidence to reject the null hypothesis.

Confidence Intervals We also compared the empirical coverage of the theoretical confidence intervals. For each data point in the validation set, the theoretical confidence interval corresponding to the fitted distribution of $\log T_i \sim \mathcal{N}(\mu(x_i), \sigma^2(x_i))$ were calculated using

$$\text{CI}_\alpha(x_i) = [\mu(x_i) \pm z_\alpha \sigma(x_i)]. \quad (4)$$

The following proportion

$$\frac{1}{N} \sum_i \mathbb{1}_{\log T_i \in \text{CI}_\alpha(x_i)} \quad (5)$$

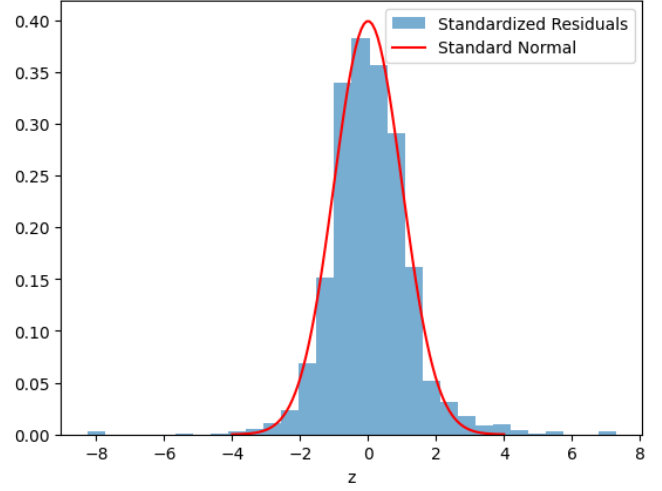


Figure 5: Comparison between standardized residual and standard normal distribution.

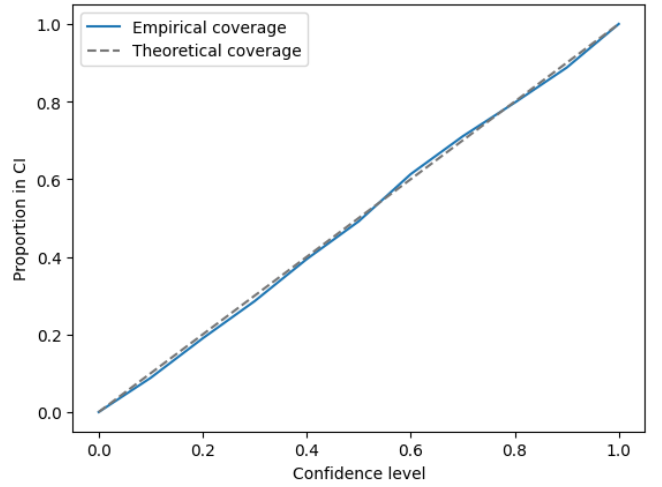


Figure 6: Comparison of theoretical and empirical confidence interval coverages at different α levels, for the test data.

was then plotted in Figure 6. We can notice that the empirical curve closely follows the theoretical coverage for each confidence interval, which confirms the validity of the model.

QQ-plot Finally, we analyzed the QQ-plot comparing the theoretical quantiles for the standard normal distribution with the sample quantiles of the standard residuals z_i for the test set. In Figure 7, the closeness with the 45-degree line (in red) suggests that the data is consistent with a standard normal distribution for most of the data. We also observe some deviations at both tails, suggesting more extreme values than expected for a standard normal. This is consistent with Figure 5, where we observe a few outliers around ± 8 . However, the deviation on the lower tail only appears under a theoretical quantile of -2.4 standard deviations, corresponding to only 0.81% of the data. This indicates that in 0.81% of cases, the fitted probabilistic model underestimated the risk of T being lower than its expected value. Such occurrences remain rare,

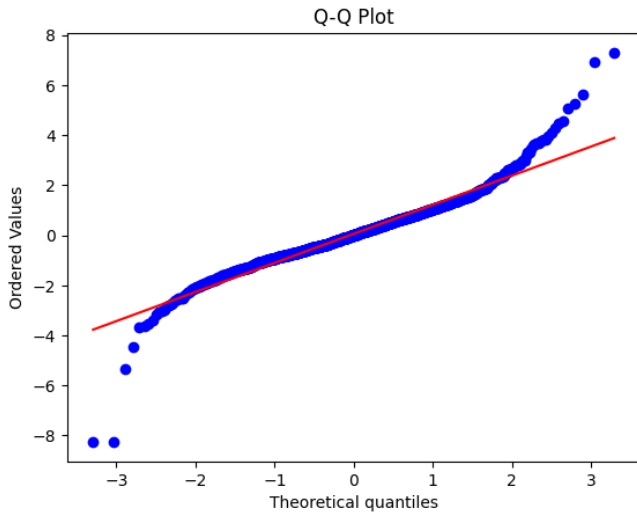


Figure 7: Q-Q-plot for the test standardized residuals.

and this heavier tail is acceptable for our application. Similarly, the upper tail suggests that the model overestimated the risk in 2.3% of cases, and such a conservative approach is also acceptable here. Considering the overall good fit for the majority of the data as well as the result of the Kolmogorov-Smirnov test, we can conclude that the neural network accurately predicts the parameters of a log-normal distribution modeling the first hitting time.

RESULTS

Influence of individual parameters

In order to analyze the variations in first hitting time resulting from changes in input values, we ran a Monte-Carlo simulation using the previously-trained probabilistic model to extract the expected value of T in each case. The results of this Monte-Carlo simulation are analyzed in the next paragraphs.

Impact of individual parameters First, the expected first hitting times were averaged over all the simulations and plotted against individual parameters, as shown in Figure 8. A qualitative analysis of those results is presented below:

- **Initial height** We observe a relatively linear increase in first hitting time with respect to the initial height h , with a difference of 1.5 s in average between initial heights of 5 ft and 50 ft. This is a significant difference that highlights the potential benefits of a higher initial height when practicing hovers with inexperienced student pilots, to provide the instructors with additional time to react to hazardous situations. However, other operational limits, such as those defined by the Height-Velocity diagram, must also be taken into account in actual operations.
- **Slope angle** Figure 8 suggests that a moderate slope up to 10 degrees does not significantly affect the value of

the first hitting time. However, for ground slopes greater than 10 degrees, the average first hitting time starts to drop significantly, decreasing from 4.5 s at 10 degrees to about 2.5 s for a slope of 25 degrees. This significant decrease highlights the importance of specific training for high-slope operations.

- **Vertical speed** Increasing the vertical rate linearly decreases the value of the first hitting time, at a rate of approximately 0.5 s per 1000 fpm. This impact is not as significant as the other parameters, and small variations in the vertical speed during a hover or landing seem unlikely to significantly increase the risk of dynamic rollover.
- **Cyclic inputs** The impact of the lateral and longitudinal cyclic input appear to be similar, with a parabolic trend reaching a maximum close to neutral (trimmed) inputs. Small variations ($\pm 5 - 10\%$) around this equilibrium do not significantly affect the first hitting time T , which suggests that keeping moderate control inputs during near-ground operations is recommended to mitigate the risk of dynamic rollovers. Moreover, we can notice that the first hitting time is slightly less sensitive to variations in longitudinal cyclic inputs than in variations of lateral cyclic inputs.
- **Collective input** The collective input appears to be the most critical variable affecting the value of the first hitting time. In Figure 8, we can observe that the average value of T ranges from 2 s to 6 s for collective inputs between -30% and $+30\%$. Thus, we can recommend that this parameter be managed by the flight instructor during the first hover practices, as a student mistake in this context could dramatically increase the risk associated with dynamic rollovers.

The other parameters used for the Monte-Carlo simulation and not shown in Figure 8 did not exhibit any major trend when plotted against the average first hitting time. Since we concluded in the previous section that these variables have a significant impact on the value of T , the lack of evident trends suggests that their effect is correlated to one or multiple other parameters. Thus, we analyze the impact of pairs of parameters on the first hitting time values in the next paragraph.

Parameter interactions In addition to the analysis of individual impacts, we also considered potential interactions between pairs of parameters. To do so, we analyzed the average first hitting time for pairs of values of specific parameters and searched for additional patterns that did not appear in the univariate analysis. The following interactions were identified:

- **Slope and height** Figure 9 features a clear interaction between the slope and height parameters. We observe that for high initial heights, close to 50 ft, the impact of the ground slope angle remains rather limited as the average

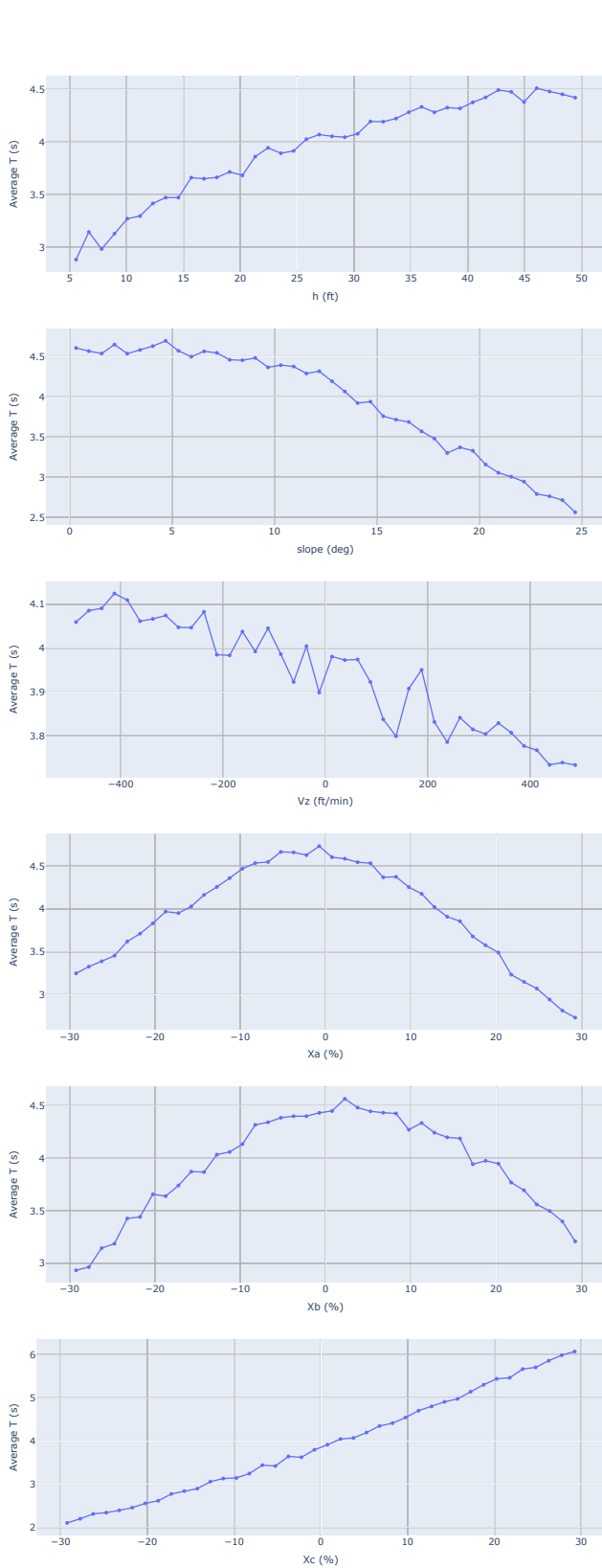


Figure 8: Average evolution of the first hitting time T with respect to individual parameters.

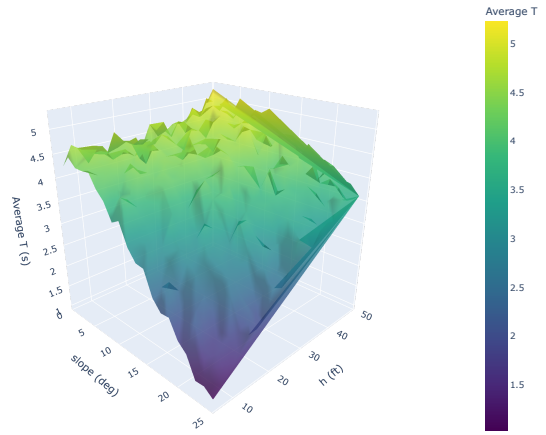


Figure 9: Average first hitting time for different slope angles and initial heights.

T varies from 5.1 s to 3.9 s for slopes of 0° to 25° , respectively. However, as the initial height decreases, the gradient of T with respect to the slope angle increases dramatically, and we observe that the trend shifts from a relatively linear relationship to a quadratic decrease in T . Thus, a ground slope of 25° coupled with an initial height of 10 ft results in a first hitting time just above 1 s, highlighting a high-risk situation for which pilot errors could quickly become critical.

- Ground slope and lateral cyclic** In Figure 10, we observe that for ground slopes under 10° , the impact of the lateral cyclic input X_a stays relatively unchanged, with a parabolic evolution of the first hitting time as described in the previous section and shown in Figure 8. However, past that 10° threshold, the maximum first hitting time value starts to decrease significantly and the value of T appears more constant across the range of X_a . We can see that for the highest ground slopes (20° to 25°), the range of values of T for $X_a \in [-30^\circ, 30^\circ]$ is less than 1 s. This completes the analysis presented in (Ref. 6), which highlighted the existence of a safe control volume, by demonstrating how different ground slopes affect, and potentially negate, the safer area defined for a specific first hitting time threshold.
- Ground slope and collective input** The warped plane shown in Figure 11 shows that the interaction between the ground slope angle and the collective input X_c mainly affects the rates at which the first hitting time T varies. For instance, we observe that for a fixed slope angle, T increases more quickly if the value of the slope is closer to 0° . The same observation holds for fixed collective inputs, as the rate of decrease in T with respect to the slope increases for higher values of X_c . It is interesting to note, however, that a higher value of X_c results in a higher first hitting time in general, whatever the angle of the slope. This might sound surprising as the Helicopter Flying Handbook (Ref. 1) describes a higher collective input as a risk factor for dynamic rollovers, but it is im-

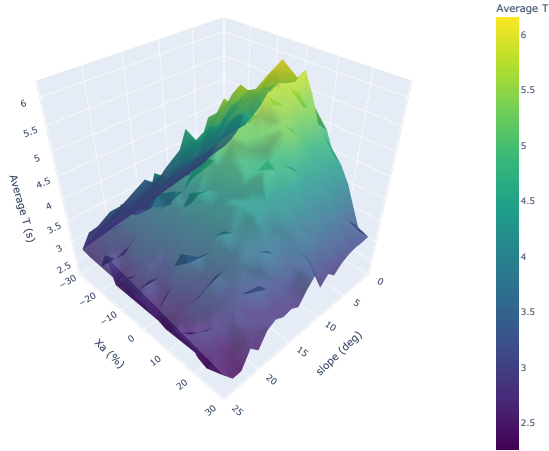


Figure 10: Average first hitting time for different slope angles and lateral cyclic inputs X_a .

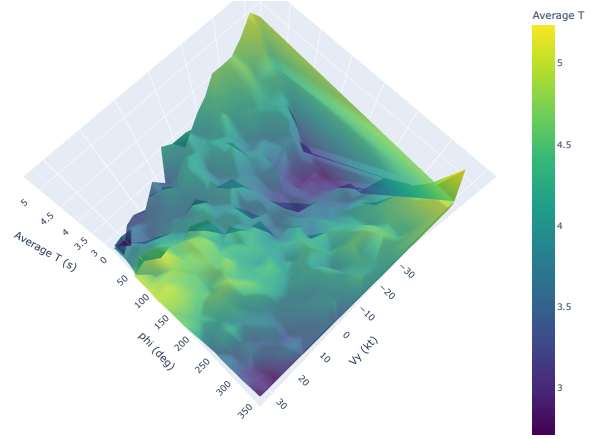


Figure 12: Average first hitting time for different slope orientations ϕ and lateral velocities V_y .

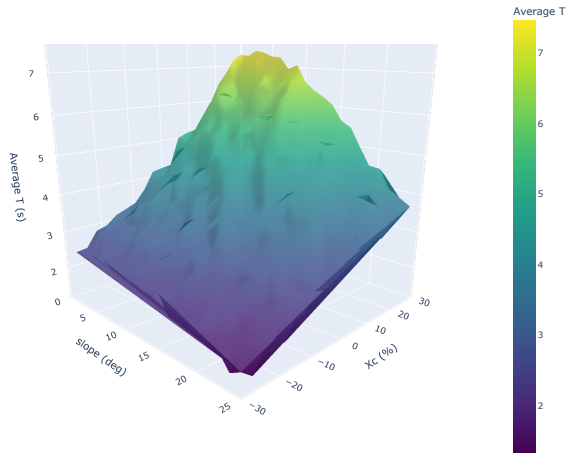


Figure 11: Average first hitting time for different slope angles and collective inputs X_c .

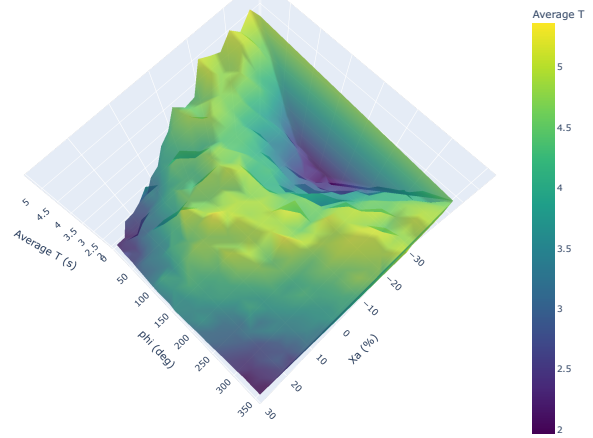


Figure 13: Average first hitting time for different slope orientations ϕ and lateral cyclic inputs X_a .

important to remember that we are studying the case of a near-ground, *in-flight* scenario, such as a hover practice. In the specific case of the helicopter taking-off with a stuck landing gear, it is still expected that a higher collective would increase the risk of dynamic rollover.

- In addition to the slope angle, the relative orientation of the ground slope with respect to the helicopter also presents interactions with other parameters. In Figure 12, we can see the interaction with the lateral velocity of the helicopter V_y . The shape of the surface is rather intuitive, as a right lateral velocity ($V_y > 0$) would result in a riskier situation (lower T) when the upslope is also to the right ($\phi \approx 0^\circ$), and a safer situation (higher T) if the right side corresponds to a downslope ($\phi \approx 180^\circ$). We can notice that the highest values for T are achieved when the helicopter flies in the downslope directions. This interaction plot seems particularly interesting in the case of slope landings, as it suggests that a safer approach would minimize the lateral velocity, or even present a slight motion away from the slope, with the helicopter landing perpen-

dicularly to the slope. Of course, this analysis only accounts for the lateral velocity and the orientation of the helicopter with respect to the ground, and additional parameters need to be accounted for in actual operations.

- Finally, we also noticed an interaction between the orientation of the ground slope ϕ and the lateral cyclic input X_a . This interaction is displayed in Figure 13. We notice that the evolution of T with respect to X_a remains similar to the one depicted in Figure 8, with the exception that the maximum value is shifted to the left (resp., right) when the upslope side is on the right (resp., left) side of the helicopter. Thus, at constant ϕ , it is generally safer to have a moderate lateral cyclic input in the downslope direction.

Probabilistic analysis

Even though the analysis conducted on the average first hitting time output of the model reveals interesting trends and

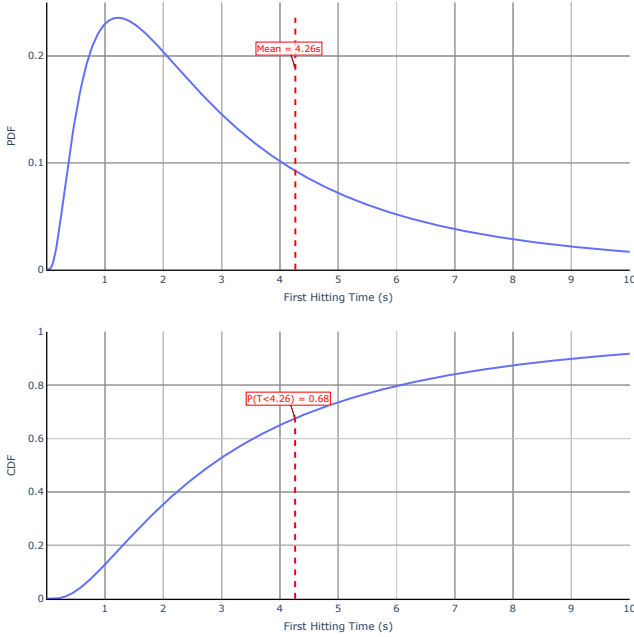


Figure 14: Example distribution of T , predicted by the probabilistic model for a fixed set of parameters.

interactions, the strength of our approach resides in the ability to predict the distribution of T for specific parameters. Due to additional external variables, such as the wind, the first hitting time value could vary greatly for a single set of inputs. For instance, Figure 14 shows an example of a predicted distribution of T for an helicopter flying at an initial height of 25 ft over a 15° left ground slope, with a left velocity of 14 kt and a slight forward cyclic input. We can see that despite a mean value of 4.26 s, the cumulative distribution function shows that in about 68% of cases, the actual value of the first hitting time will be lower. More importantly, in 25% of cases, this value will be less than 1.5 s, which likely constitutes an unsafe situation, as opposed to what the mean of T initially suggested. Such findings highlight the need for a probabilistic safety metric to complete the first hitting time in dynamic rollover prediction. To do so, our approach starts by defining a critical first hitting time threshold T_c , as suggested in previous work (Ref. 6), that will depend on the type of operations to be conducted. Then, a regression model is created to predict the CDF value at $T = T_c$ for different values of the input parameters, thus estimating $P(T \leq T_c)$, the risk of the actual first hitting time being lower than the selected threshold. Finally, using this regression model, this risk is displayed on contour plots to identify the safer conditions. The rest of this section showcases a use-case analyzing the estimated risk for a threshold $T_c = 2.8$ s with various initial conditions, and the results are shown on contour plots for different cyclic inputs. As an example, an acceptable risk of 5% was used to display the critical boundaries in Fig. 15 to 19.

Figure 15 shows the probability of $T \leq 2.8$ s for the baseline case in which the helicopter has no lateral or longitudinal velocities, starts with an initial height of 25 ft, and the ground features a slight slope of 2° with the upslope to the left of

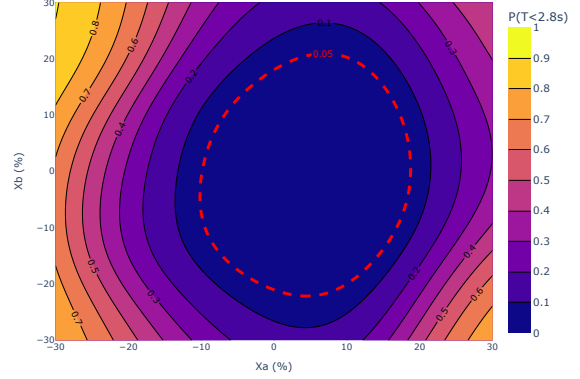


Figure 15: Contour plot showing the risk $P(T \leq T_c)$ for different cyclic inputs. The dotted red line shows the safe region for an acceptable risk of 5%.

the helicopter. The collective input is $X_c = 0$, which corresponds to the trimmed input for a hover scenario. We observe that the critical boundary showing the safe cyclic inputs in these conditions, defined by the critical threshold $T_c = 2.8$ s and the acceptable risk level of 5%, is wide and rather circular. We can see that it is slightly shifted towards positive values of X_a , which corresponds to a right cyclic input and is consistent with the slight ground slope. When we increase the slope angle to 10° (Fig. 16), we can see that the contour plot becomes asymmetric, with right cyclic inputs generally safer than left cyclic inputs. Indeed, the yellow area on the left side of the plot indicates that high left cyclic inputs would almost certainly result in a first hitting time lower than the chosen threshold of 2.8 s. For the specific risk of 5% used to display the critical boundary, the changes in safe controls is not significant, except that the safe area seems to have slightly shrunk. If we had chosen an acceptable risk of 20%, however, we can see that the shape of the critical boundary would have shifted significantly, by allowing higher right lateral cyclic inputs, up to $X_a = 30\%$, as long as the longitudinal cyclic input X_b remains moderate (roughly less than $\pm 10\%$).

Moreover, Figure 17 shows how changing the orientation of the 10° slope relative to the helicopter affects the riskiness of the cyclic controls. Compared to Figure 16, the upslope side was moved from the left side of the helicopter to its front side. As a result, the safe region was recentered with respect to X_a and shifted to positive values of the longitudinal cyclic input X_b , which correspond to backward cyclic inputs for the pilots. It is also interesting to note that the safe area shrank, suggesting a lower risk of quick dynamic rollover when flying perpendicularly to the slope rather than facing the upslope direction.

If we also add a longitudinal motion toward the ground ($V_x = 10$ kt), we observe in Figure 18 that the the safer area shrinks dramatically, indicating an increased risk in this situation. We can note that the shape of the contours does not changes significantly compared to Figure 17, which shows

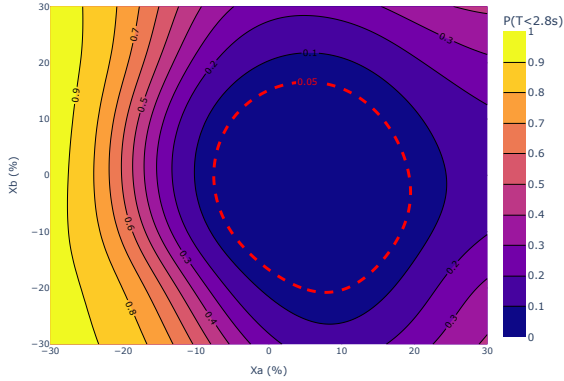


Figure 16: Modified contour plot for an increased slope angle (10°).

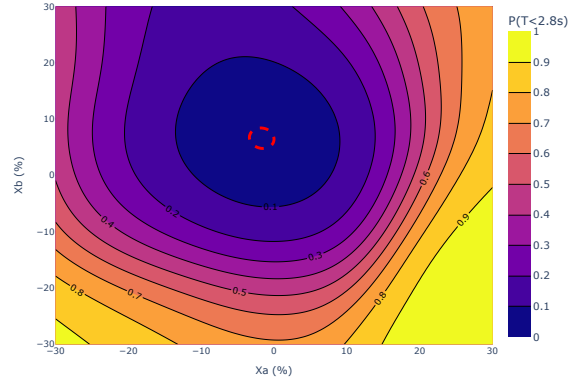


Figure 18: Contour plot for a 10° front upslope, and an additional 10 kt forward velocity.

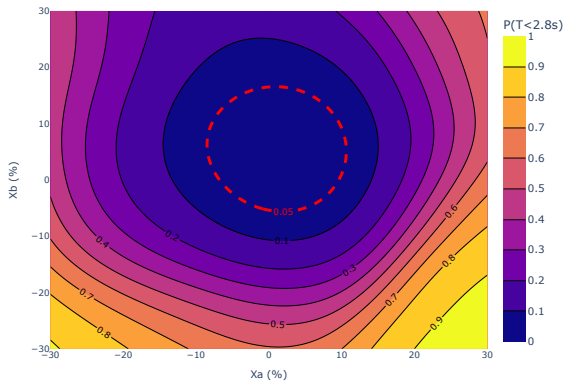


Figure 17: Modified contour plot for a front upslope (10°).

that the risk increased uniformly for every pair of cyclic inputs.

Finally, this risk could easily be mitigated by increasing the initial height of the helicopter from 25 ft to 35 ft, as shown by Figure 19. In that case, we see that the risk decreased for all cyclic inputs, and the safe area widened significantly. This reinforces the general principle that near-ground operations should be practiced at higher heights, within operational limits, to mitigate the risk of dynamic rollover. This is particularly important with inexperienced student pilots, as even a few feet of additional height can significantly improve the margin for recovery.

CONCLUSION

This paper introduced a probabilistic approach to the analysis of dynamic rollovers. By predicting the distribution of first hitting times for a range of initial conditions in near-ground helicopter flight, we demonstrated the limitations of using a deterministic metric in the assessment of dynamic rollover risks. We used that distribution to derive a probabilistic metric and identify a range of safer conditions with regard to dy-

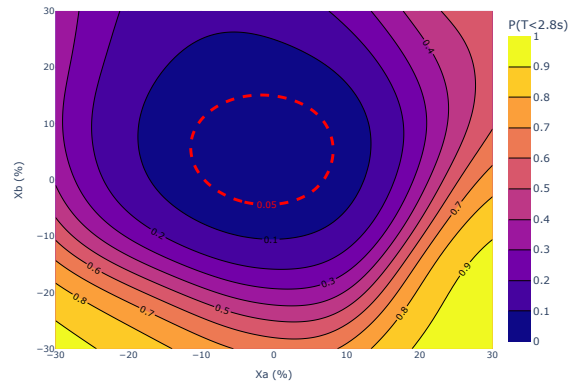


Figure 19: Contour plot for a 10° front slope, a 10 kt forward velocity, and an increased height of 35 ft.

amic rollovers. The impact of key variables was analyzed, highlighting their interactions and individual effects on the likelihood of rapid dynamic rollover onset. When applied to real-world flight data, this approach has the potential to improve HFDM systems by providing safety insights to operators.

Author contact: Ilias Baali (ibaali3@gatech.edu), Alexia P. Payan (alexia.payan@gatech.edu), Charles C. Johnson (charles.c.johnson@faa.gov), and Dimitri N. Mavris (dimitri.mavris@aerospace.gatech.edu).

ACKNOWLEDGMENTS

The work presented here is funded by the Federal Aviation Administration through PEGASAS (Partnership to Enhance General Aviation Safety, Accessibility and Sustainability), FAA Center of Excellence on General Aviation, Project No. 2: Rotorcraft Aviation Safety Information Analysis and Sharing (ASIAS). Project No. 2: Rotorcraft ASIAS is a partnership between PEGASAS researchers at the Georgia Institute of Technology, the FAA, Vertical Aviation International (VAI),

and other partners. The information presented in this paper and contained in this research does not constitute FAA Flight Standards or FAA Aircraft Certification policy.

REFERENCES

1. Federal Aviation Administration, *Helicopter Flying Handbook*, U.S. Department of Transportation, Federal Aviation Administration, Washington, D.C., FAA-H-8083-21B, 2019.
2. Payan, A. P., Gavrilovski, A., Jimenez, H., and Mavris, D. N., "Improvement of Rotorcraft Safety Metrics Using Performance Models and Data Integration," *Journal of Aerospace Information Systems*, Vol. 14, (1), 2017, pp. 26–39. DOI: 10.2514/1.I010467.
3. Chin, H.-J., Payan, A. P., Mavris, D., and Johnson, C., *Knowledge Discovery within ADS-B Data from Routine Helicopter Tour Operations*. DOI: 10.2514/6.2020-2872.
4. Chin, H.-J., Payan, A. P., Johnson, C. C., and Mavris, D. N., "Anomaly Detection in Initial Climb Segments for Helicopter Operations," Proceedings of the Vertical Flight Society's 77th Annual Forum & Technology Display, May 2021.
5. Robinson, J. N., Payan, A. P., Johnson, C., and Mavris, D. N., "Improved Instrument Approach Stability Analysis for Helicopters Using Data Fusion and Analytics," *Journal of Aerospace Information Systems*, Vol. 19, (11), 2022, pp. 729–746. DOI: 10.2514/1.I011076.
6. Gavrilovski, A., *Predictive Helicopter Flight Data Monitoring for Flight Safety Design*, Ph.d. thesis, Georgia Institute of Technology, Atlanta, GA, May 2017.
7. Huan, X., Jagalur, J., and Marzouk, Y., "Optimal experimental design: Formulations and computations," *Acta Numerica*, Vol. 33, 2024, pp. 715–840. DOI: 10.1017/S0962492924000023.
8. Parmar, A., Katariya, R., and Patel, V., "A Review on Random Forest: An Ensemble Classifier," International Conference on Intelligent Data Communication Technologies and Internet of Things (ICICI) 2018, edited by J. Hemanth, X. Fernando, P. Lafata, and Z. Baig, 2019.
9. Louppe, G., *Understanding Random Forests: From Theory to Practice*, Ph.D. thesis, 2015.
10. Lundberg, S. M., and Lee, S.-I., "A Unified Approach to Interpreting Model Predictions," *Advances in Neural Information Processing Systems*, edited by I. Guyon, U. V. Luxburg, S. Bengio, H. Wallach, R. Fergus, S. Vishwanathan, and R. Garnett, Vol. 30, 2017.